CONF-890379--2

DE89 012332

The High-Energy Transport Code HETC88*

R. G. Alsmiller, Jr.
F. S. Alsmiller
T. A. Gabriel
O. W. Hermann
J. M. Barnes

* Research sponsored by Office of High Energy and Nuclear Physics, U.S. Department of Energy under contract number DE-AC05-84OR21400 with Martin Marietta Energy Systems, Inc.

Acknowledgement

The authors thank D. Groom of the SSC Central Design Group for many helpful discussions, particularly those concerned with the Tevatron experiment.

Abstract

An upgraded version, HETC88, of the previously available High-Energy Transport Code HETC is briefly described. In the upgraded code, the particle production model from hadron-nucleus nonelastic collisions at energies greater than 5 GeV has been revised. At nucleon and pion energies below 5 GeV, HETC88 is not different from the code previously available. In particular, provision is still made to allow neutrons with energies $\leq$20 MeV to be transported by one of the available codes designed for low-energy neutron transport.

Calculated results for the longitudinal distribution of the flux of neutrons with energy $\geq$40 KeV in the Tevatron tunnel when 900 GeV protons interact with N_2 in a warm section are presented and compared with experimental data. Some disagreements between the calculated and measured neutron flux are found. For 20 TeV protons incident on a large cylindrical iron target, calculated "star" density results from HETC88, FLUKA87, CASIM, and MARS10 are also compared.

1. INTRODUCTION

The High-Energy Transport Code HETC[1] has been available for many years and has been used in a wide range of applications. Results obtained with the code have been compared with a variety of experimental data and reasonable results have usually been obtained.[2,3] At the higher energies of the proposed Superconducting Super Collider (SSC), the scaling model used in the code to describe particle production from hadron-nucleus collisions is, at best, very approximate. Since this model was developed, a large amount of expermiental and theoretical work has been done and more reliable models are now available. In particular, a multi-chain fragmentation model of hadron-nucleus collisions has been developed and implemented into a Monte Carlo code by J. Ranft et al., (see Ref. 4 and the references given therein) following the work of A. Capella et al., (see Ref. 5 and the references given therein). In the present paper, an upgraded version of HETC, called HETC88, that utilizes a slightly modified version of this collision model[6] is described and a comparison between calculated results and experimental data is presented.

In Section 2 the modifications that have been made to HETC to produce HETC88 are described and discussed. In Section 3 calculated results for the longitudinal distribution of the flux of neutrons with energy $\geq$ 40 KeV in the Tevatron tunnel when 900 GeV protons interact with N_2 in a warm, i.e. non-cryogenic, section of the Tevatron are presented and compared with experimental data.[7,8] In Section IV calculated star densities as a function of position obtained with HETC88, FLUKA87,[9] CASIM[10,11] and MARS10[12,13] are compared for the case of 20 TeV protons incident on a large iron cylinder.

2. THE HIGH-ENERGY TRANSPORT CODE HETC88

The High-Energy Transport Code (HETC) has been described in detail previously,[1-3] so only a brief discussion of the general code will be given here and emphasis will be given to those parts of the code that have been revised. In the remainder of this paper the code described in Refs. 1-3 will be referred to as HETC72 and the latest version of the code that was used in obtaining the results presented here will be termed HETC88.

Basically, HETC72 and HETC88 are analogue Monte Carlo codes that are designed to study the nucleon-meson cascade that develops when high-energy ($\lesssim$20 TeV) nucleons and pions pass through matter. In these codes protons, charged

pion, and muons are transported until they undergo nuclear reaction, decay, or escape from the system. Neutrons are transported similarly, but a neutron whose energy is less than 20 MeV is stored so that it may be transported with one of the codes designed for such low-energy neutron transport, e.g., MORSE.[15] Neutral pions are also stored so that the photons from their decay may be transported by an electron-photon cascade code such as EGS.[16]

A unique feature of both HETC72 and HETC88 is that cross section models are used rather than cross section data. That is, when a high-energy nonelastic nucleon-nucleus or pion-nucleus collision occurs, a cross section model is used to determine the type, energy, and angle of the emitted particles. The only difference between HETC72 and HETC88 is that the cross section model used to predict particle production from nonelastic collisions at energies $\geq$ 5 GeV has been changed.

The model used in HETC88 is that described and compared with experimental data in Ref. 6. As discussed in Ref. 6 this model is a slightly modified version of the model developed by J. Ranft et al. (see Ref. 4 and the references given therein), that is, available in the transport code FLUKA87.[9]

Since this model is available as a Monte Carlo code, its incorporation into HETC72 was straightforward except for the fact that the model includes the production of a variety of mesons and baryons other than the nucleons and pions that are considered in HETC72. In HETC88, these additional particles were at the point of their production converted to nucleons and pions. In the conversions, positively, negatively, and neutral mesons were converted to π^+, π^-, and π° mesons, respectively, and charged and neutral baryons were converted to protons and neutrons, respectively. In each conversion, the total energy and direction of motion of the original particle was retained. This is a very approximate procedure, but it should not lead to appreciable error because the number of particles that must be converted in a Monte Carlo history is not large compared with the number of particles produced in the history.

3. COMPARISON OF CALCULATED AND EXPERIMENTAL DATA (>40 KeV) LEVEL IN THE TEVATRON

In a recent experiment, the longitudinal distribution of neutron flux in the Tevatron tunnel was measured.[7,8] A controlled N_2 gas leak was introduced near the center of a warm section and the neutron flux was measured near the wall of the tunnel as a function of distance from this gas leak. In an earlier report,[8]

report,[8] calculated results were presented and compared with this experimental data and some disagreements were found. In these earlier calculations, several simplifying assumptions were made, e.g., a point source and cylindrical symmetry, and a preliminary version of HETCS8[17] was used. The calculations have now been completed with the upgraded HETCS8 and with many of the simplifying assumptions removed. In this section, these revised calculations are discussed and the results compared with the experimental data.

In Fig. 1 a schematic diagram of a cross section of the Tevatron tunnel is shown with the position of the Bonner sphere that was used in the measurements shown. In the calculations reported here, this cross section, i.e. the main ring and Tevatron, tunnel wall, etc., was simulated as shown using the combinatorial geometry routines in HETCS8. The Tevatron magnets were modeled using information in Ref. 18, and the magnetics of the main ring were modeled as iron using information supplied by J. D. Cossairt.[19] Longitudinally, i.e., in the direction of the proton beam, the warm section is 11.8 m long with the nitrogen leak at its center. The main ring was assumed to be continuous and straight in the longitudinal direction, i.e., all effects of the curvature of the tunnel are neglected, and the Tevatron magnets were assumed to be continuous and straight in the longitudinal direction, except in the region of the warm section where there is no magnet. The sources of the calculations were the interactions between the 900 GeV proton beam and the nitrogen nuclei in the warm section. The variation of the gas pressure and thus the number of interacting protons was taken to vary linearly between the center and ends of the warm section. In the beam pipe in the vicinity of the Tevatron magnets, a magnetic field of 38.5 T was used in the calculations since this field will have a significant effect on the charged particles, but no magnetic field is assumed in the magnet structure.

The low energy ($\leq$20 MeV) neutron transport was carried out using MORSE[15] with cross section data from the VITAMIN-E library.[20,21] The geometry and material configurations used in MORSE are the same as those used in HETCS8.

In Fig. 2 the calculated and experimental flux of neutrons with energy $\geq$40 KeV are compared as functions of distance from the gas leak. The error bars on the calculated data are statistical and represent one standard deviation. The peak in the calculated results is larger than the peak in the experimental data by approximately a factor of 2 and the peak in the calculated results occurs at a distance of approximately 5 m closer to the source of the gas leak (the 0 of

distance in Fig. 2) than does the experimental peak. The calculated results in Fig. 2 are normalized per interacting proton. The normalization of the experimental data in Fig. 2 is that given in Ref. 8, but the uncertainty in this normalization is now thought to be of the order of a factor of 2.[22] Thus, the disagreement in magnitude shown in Fig. 2 may not be real, but there is, at present, no satisfactory explanation for the disagreement in the longitudinal position of the peak of the calculated and experimental neutron flux distributions. It should be noted that the peak of the calculated distribution in Fig. 2 is centered about the entrance to the Tevatron magnet immediately following the source. The magnetic field causes the high energy charged hadrons from the source to strike the magnet near its entrance so a peak in the vicinity of the entrance is to be expected, but just how close to the entrance this peak should be is not very certain.

4. 20 TeV PROTONS INCIDENT ON A LARGE IRON CYLINDER

At the energies of interest to the proposed Superconducting Super Collider, there are no experimental measurements, but all of the codes HETC88, FLUKA87,[8] CASIM,[9,10] and MARS10[11,12,13] are capable of carrying out calculations at these energies. In this section calculated results for 20 TeV protons incident along the axis of a large iron cylinder from each of these codes are compared. The results from HETC88 and FLUKA87 were obtained at ORNL and the results from CASIM and MARS10 are taken from Ref. 14.

The cylindrical target has a radius of 100 cm and a length of 500 cm. The proton beam was incident along the axis of the cylinder and had a spot size which is Gaussian with a standard deviation of 5 mm. The quantity which is calculated and compared is the radial distribution of star density over a depth interval of 80 to 100 cm and the radial distribution of star density integrated over all depths, i.e., from 0 to 500 cm. A star is defined as any nonelastic collision produced by a particle with momentum greater than 0.3 GeV/c, so the low-energy particles are not involved in the comparison here. This is necessary because the FLUKA87, CASIM and MARS10 programs do not attempt to calculate the low-energy neutrons.

The calculated results are shown in Fig. 3. In the case of the CASIM only a few of the many data points that are given in Ref. 14 are given in Fig. 3; basically a smooth curve drawn through the points shown gives a very good representation of the CASIM results. In the depth interval of 80 to 100 cm the calculated results from all of the codes are in quite good agreement. In the case of the integration over all depths, all of the results are in quite good agreement at the small ($\leq$25

cm) radii, show some significant differences at intermediate (25 to 60 cm) radii, and tend to agree again at the larger radii. In general, HETCSS gives the lowest longitudinally integrated value at a given radius and CASIM gives the highest longtitudinally integrated value at any r. The quantities compared in Fig. 3 are very integral quantities; when more detailed comparisons are made larger differences may be obtained.

5. REFERENCES

1. Chandler, K C. and Armstrong, T. W. "Operating Instructions for the High-Energy Nucleon-Meson Transport Code HETC," Oak Ridge National Laboratory, ORNL-4744, Oak Ridge, TN (1972).
2. Armstrong, T. W. et al., "Monte Carlo Calculations for High-Energy Nucleon-Meson Cascade and Comparison with Experiment," Nucl. Sci. Eng. 49, 82 (1972).
3. Alsmiller, R. G. Jr., "Nucleon-Meson Transport Calculations," Spallation Nuclear Reactions and Their Applications, Edited by B. S. P. Shen and M. Merkeer, Vol. 59, 1976, D. Reidel Publishing Co., Dordrecht-Holland/Boston U.S.A.
4. Ranft, J. and Ritter, S. "Rapidity Ratios, Feynman-x Distributions, and Forward-Backward Correlations in Hadron-Nucleus Collisions in a Dual Monte Carlo Multi-Chain Fragmentation Model," Z. Phys. C. - Particles and Fields 27, 569 (1985).
5. Capella, A. and J. Tran Thanh Van, "Hadron-Nucleus Interactions and the Leading Particle Effect in a Dual-Parton Model," Z. Phys. C. - Particles and Fields 10, 249 (1981).
6. Alsmiller, F. S. and Alsmiller, R. G. Jr., "Inclusion of Correlations in the Empirical Selection of Intranuclear Cascade Nucleons from High-Energy Hadron-Nucleus Collisions," Oak Ridge National Laboratory, ORNL/TM-11032 (1989) (submitted to Nuclear Instruments and Methods in Physics Research).
7. Cossairt, J. D. et al., SSC Central Design Group Report, in preparation (1987).
8. Gabriel, T. A. et al., "Preliminary Simulation of the Neutron Flux Levels in the Fermilab Tunnel and Proposed SSC Tunnel," Superconducting Super Collider, SSC-110 (1987).
9. Aarnio, P. A. et al., "Enhancements to the FLUKA86 Program (FLUKA87)," European Organization of Nuclear Research, TIS-RP/190 (1987).
10. Van Ginneken, A. "CASIM: Program to Simulate Transport of Hadronic Cascades in Bulk Matter, Fermilab Report FN-272 (Fermilab, Batavia, Illinois) (1975).
11. Cossairt, J. D., Butata, S. M. and Gerardi, M. A. "Absorbed Dose Measurements at an 800 GeV Proton Accelerator: Comparison with Monte Carlo Calculations," Nucl. Instrum. & Methods in Phys. Res. A238, 504 (1985).

12. Kalinovsky, A. N., Mokhov, N. V. and Nikitin, Yu P. "Penetration of High Energy Particles through Matter," Energoatomizdat (1985) (in Russian, 1989 in English).
13. Mokhov, N. V. "The MARS10 Code System: Inclusive Simulation of Hadronic and Electromagnetic Cascades and Muon Transport," Fermi National Accelerator Laboratory, FN-509 (1989).
14. Mokkov, N. V. and Cossairt, J. D. "A Short Review of Monte Carlo Hadronic Cascade Calculations in the Multi-TeV Energy Range," Nucl. Instrum. & Methods in Phys. Res. A244 (1986).
15. Emmett, M. B. "The MORSE Monte Carlo Radiation Transport System," ORNL-4972, Oak Ridge National Laboratory (1975).
16. Ford, R. L. and Nelson, W. R. "The EGS Code System: Computer Program for the Monte Carlo Simulation of Electromagnetic Cascade Showers (Version 3)," Stanford Linear Accelerator Center, SLAC-210 (1978).
17. Alsmiller, R. G. Jr., "Modifications of the High-Energy Transport Code (HETC) and Comparisons with Experimental Results," Proceedings of the ANS Topical Conference on Theory and Practices in Radiation Protection in Radiation Protection and Shielding.
18. Cole, F. T. et al., "A Report on the Design of the Fermi National Accelerator Laboratory Superconducting Accelerator," FNAL (1979). (See also H. T. Edwards. *Ann. Rev. Nucl. Part. Sci.* **35**, 6025 (1985).
19. Cossairt, J. D. Fermi National Accelerator Laboratory, private communication, 1987.
20. Roussin, R. W. et al., "VITAMIN-E: A Coupled 174-Neuron, 38-Gamma-Ray Multigroup Cross Section Library for Deriving Application-Dependent Working Libraries for Radiation Transport Calculations," available from the Radiation Shielding Information Center, Engineering Physics & Mathematics Division, Oak Ridge National Laboratory, as DLL-11131 VITAMIN-E.
21. Santoro, R. T. et al., "Monte Carlo and Discrete Calculations of 14-MeV Neutrons Streaming Tl rough a Stainless Steel Duct: Comparison with Experiment I," *Nucl. Sci. Eng.* **91**, 584 (1986).
22. Groom, D. E., Superconducting Super Collider Central Design Group, private communication, 1988.

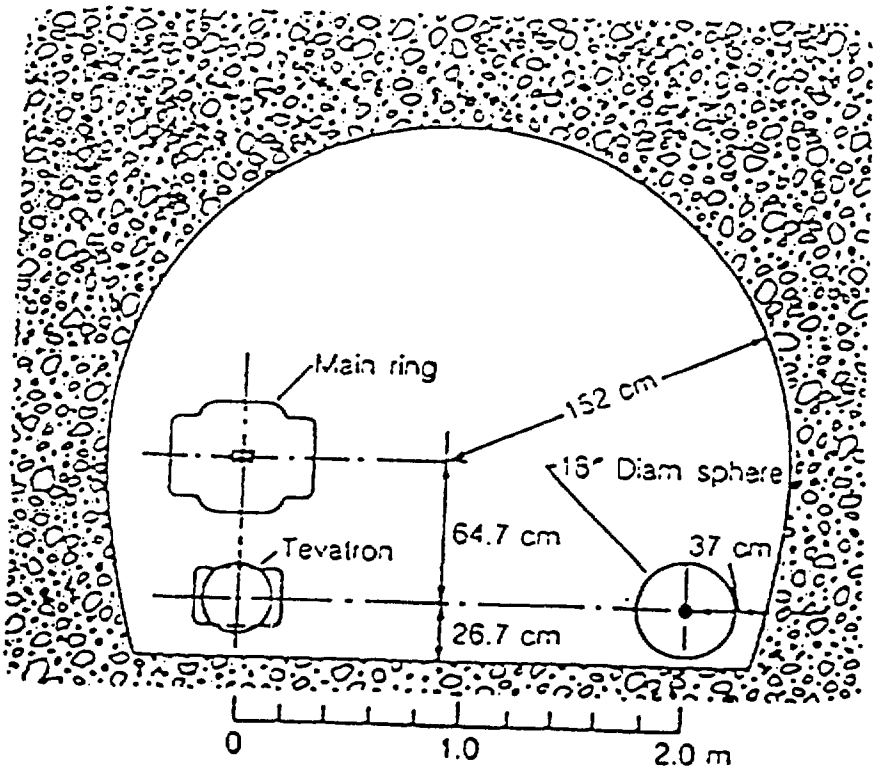

Fig. 1. Schematic cross section of Tevatron tunnel.

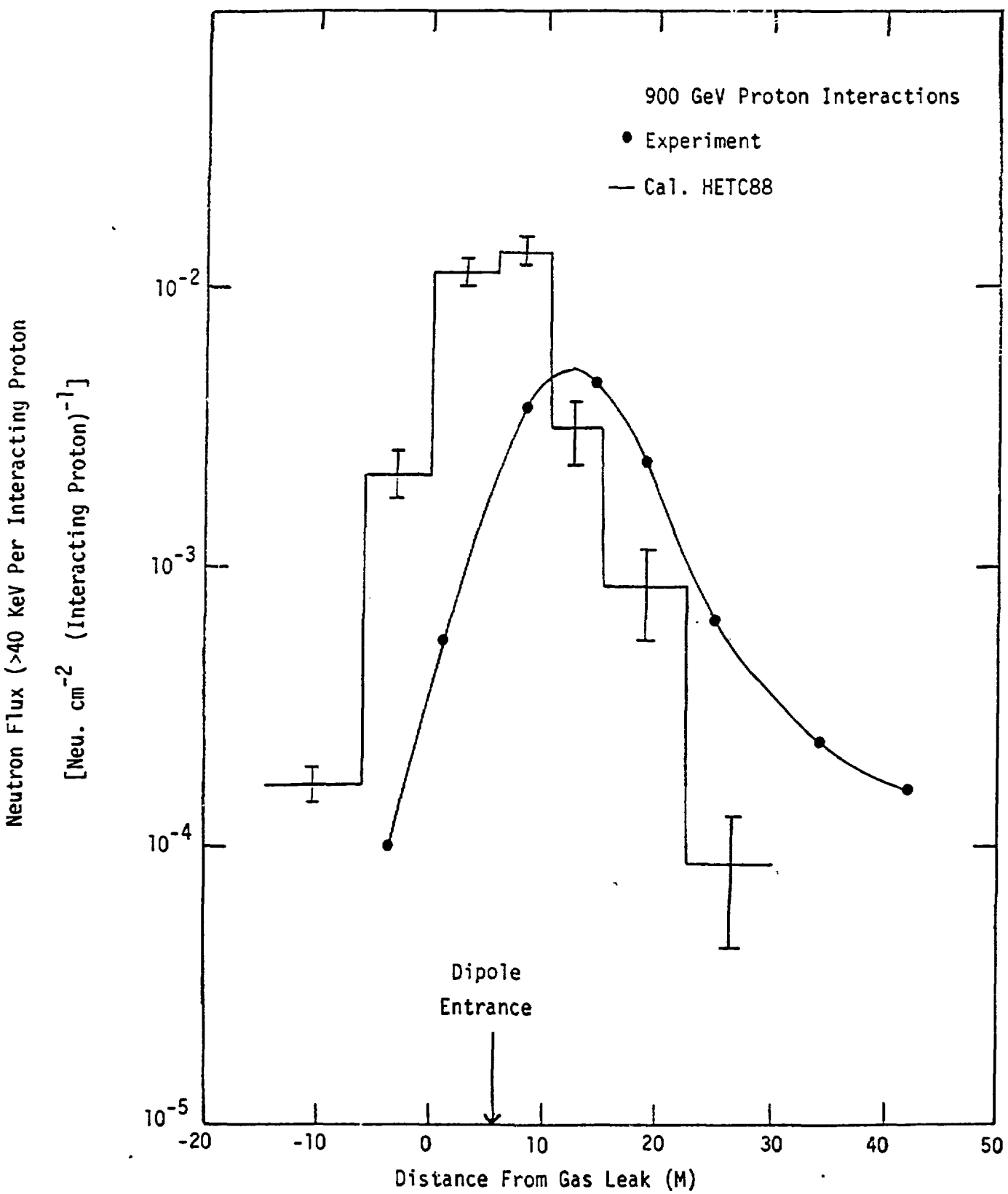

Fig. 2. Longitudinal distribution of the flux of neutrons with energy greater than 40 KeV in the Tevatron tunnel.

Fig. 3. Star density vs. radius for 20 TeV protons incident along the axis of a large iron cylinder. Results are shown for the depth interval of 80 to 100 cm (scale at left) and integrated over all depths scale at right.